Modeling solute mass exchange between pore regions in slurry-injected soil columns during intermittent irrigation

Glæsner, Nadia; Diamantopoulos, Efstathios; Diamantopoulos, Efstathios; Magid, Jakob; Kjaergaard, Charlotte; Gerke, Horst H.

Published in:
Vadose Zone Journal

DOI:
10.2136/vzj2018.01.0006

Publication date:
2018

Document version
Publisher's PDF, also known as Version of record

Published online May 24, 2018

Special Section: Nonuniform Flows across Vadose Zone Scales

Core Ideas

- Water flow and solute transport models described solute leaching during slurry injection.
- Intermittent flow increased leaching of injected slurry compounds compared with steady flow.
- Mass exchange of slurry compounds during interruptions occurred from im- to mobile pore regions.
- Mass exchange between pore regions should be included in larger scale model predictions.

Modeling Solute Mass Exchange between Pore Regions in Slurry-Injected Soil Columns during Intermittent Irrigation

Nadia Glæsner,* Efstathios Diamantopoulos, Jakob Magid, Charlotte Kjaergaard, and Horst H. Gerke

Animal slurry application to agricultural land can be a threat to the quality of groundwater and nearby surface water bodies by percolation of solutes from slurry sources. We hypothesized that local-scale processes, such as mass exchange between preferential flow paths and matrix pore regions, can play a substantial role in relation to slurry application and nutrient leaching. To improve understanding of these mass exchange mechanisms, soil column leaching data of nonreactive slurry components after injection of dairy slurry were analyzed under different initial and boundary conditions with single- and double-porosity model approaches. The data set was from nine intact soil columns (20-cm i.d., 20-cm height) of the plow layer of arable loamy topsoil that were percolated under unsaturated steady-flow conditions with a suction of 5 cm applied at the bottom. Both single- and double-porosity water flow and mobile–immobile solute transport models could describe these experimental breakthrough curves. Rainfall interruptions mimicking more natural conditions and variably saturated intermittent flow led to higher leaching of injected slurry compounds than steady-flow conditions. These observations could be explained by an increased mass exchange of dissolved injected slurry components from the immobile to the mobile pore water regions during interruptions. The results suggest that column tests under steady-flow conditions could lead to false predictions of solute leaching after slurry injection in structured soils. Furthermore, local-scale processes, such as mass exchange between pore regions, should be included in larger scale model predictions of nutrient losses from agricultural fields.

Abbreviations: 1D, one-dimensional; 3D, three-dimensional; BTC, breakthrough curve; DP-MIM, double-porosity mobile–immobile model; ^3H_2O, tritium water; PV, pore volume; RMSE, root mean square error; SP-EQ, single-porosity equilibrium model.

N. Glæsner and H.H. Gerke, Leibniz Centre for Agricultural Landscape Research (ZALF), 15374 Müncheberg, Germany; N. Glæsner, E. Diamantopoulos and J. Magid, Faculty of Science, Univ. of Copenhagen, 1958 Frederiksberg, Denmark; C. Kjaergaard, Dep. of Agroecology, Aarhus Univ., Denmark; C. Kjaergaard, current address: SEGES, Dep. of Construction and Environment, DK-8200 Aarhus N, Denmark. *Corresponding author (nadia.glaesner@gmail.com).

Received 15 Jan. 2018.
Accepted 26 Mar. 2018.
Supplemental material online.

Citation: Glæsner, N., E. Diamantopoulos, J. Magid, C. Kjaergaard, and H.H. Gerke. 2018. Modeling solute mass exchange between pore regions in slurry-injected soil columns during intermittent irrigation. Vadose Zone J. 17:180006. doi:10.2136/vzj2018.01.0006

Leaching of plant nutrients from agricultural fields is causing eutrophication problems in surface waters and contamination of groundwaters worldwide. Nutrient losses are especially high from fields subjected to land application of animal manure in areas of high livestock production (Ball Coelho et al., 2007; Kronvang et al., 2009). Among the various types of animal manure (i.e., farmyard manure, dung compost, liquid manure), slurry is a mixture of feces and urine produced by housed livestock, usually mixed with bedding material and water during farm management, resulting in liquid manure that can be pumped. Slurry dry matter content is 1 to 10% (Pain and Menzi, 2003). Slurry N and P contents are of particular environmental concern because of the risk of unintended losses by leaching or surface runoff (e.g., Glæsner et al., 2012; Liu et al., 2012).

Various soil management strategies including minimum tillage and slurry injection have been proposed to minimize the slurry-induced leaching potential. These techniques have been experimentally evaluated (e.g., Maguire et al., 2011) and assessed with simulation models (e.g., Giola et al., 2012). Injection of animal slurry into arable topsoil was proposed as an alternative to surface application to reduce NH_3 gas emissions (Rubæk et al., 1996; Webb et al., 2010) and to minimize surface runoff and nutrient losses due to leaching. Glæsner et al. (2011a, 2011b, 2011c) experimentally compared the effects of surface application and injection of slurry on leaching of nonreactive slurry solutes

and dissolved and particulate P forms for three major arable topsoil types in Denmark represented by sandy to loamy textures. Injection of dairy slurry reduced leaching of dissolved nonreactive slurry components (Glæsner et al., 2011a) as well as of dissolved and particulate P (Glæsner et al., 2011b) in the fine- to medium-textured loamy soils compared with surface application; the effect was less obvious for the coarse-textured sandy soils. These studies highlighted the complex soil pore structure effects on flow and transport properties as follows: breakthrough curves for tritium water (^3H_2O) and Br^- as conservative tracers yielded early appearance for the more loamy soils (Glæsner et al., 2011a). Early tracer appearance in the more aggregated loam indicated the effects of preferential flow (e.g., Flühler et al., 1996; Gerke, 2006) and nonequilibrium solute transport (e.g., van Genuchten and Dalton, 1986). Nonequilibrium solute transport can be explained by the existence of multiple pore systems (van Genuchten and Wierenga, 1976) characterized by mobile to immobile pore regions.

Solute transport in column experiments has often been studied assuming steady-flow conditions (de Jonge et al., 2004; Glæsner et al., 2011a), thereby simplifying model analysis by neglecting changes in the soil water content. Under steady-flow conditions, breakthrough curves of percolation experiments can be successfully described with the convection–dispersion equation. Transferring or upscaling the results of such laboratory column data to dynamic field-scale conditions can be criticized because the steady-flow assumption rarely occurs under field conditions. It is more realistic to assume rainfall infiltration periods followed by "dry" or zero-flux periods. Under unsaturated conditions, these intermittent infiltration conditions generate variably saturated flow of water (Brusseau et al., 1997; Wehrer and Totsche, 2005), which in structured, aggregated soil could lead to locally varying pore water velocities. Local mass exchange processes between more and less mobile pore water regions could thus be triggered in soil column studies by intermittent irrigation regimes (Glæsner et al., 2011c).

While diffusion-limited solute mass exchange can already occur during steady flow in structured soils, an additional mass exchange by the transfer of water between the mobile and immobile pore regions has to be considered for intermittent flow induced by intermittent irrigation regimes (e.g., Gerke, 2006; Jarvis, 2007). For the model description of this process, a number of numerical single- and double-porosity models are available (e.g., Šimůnek et al., 2003; Šimůnek and van Genuchten, 2008). The double-porosity approach assumes either a single flow domain (mobile–immobile type) or two flow domains (mobile–mobile type) such as dual-permeability models (Gerke and van Genuchten, 1993; Jarvis, 1994).

The hypothesis of the current study was that solutes from injected slurry components will quickly be transported in preferential flow paths during infiltration, thereby creating a local nonequilibrium in solute concentrations between aggregates and flow paths (e.g., Gerke et al., 2013). Subsequently, when infiltration stops, local solute concentrations could gradually approach equilibrium; and when infiltration resumes, the equilibrated soil solution of the interaggregate pores can create another solute concentration peak in the breakthrough curve before effluent concentrations decrease again until the next cycle of irrigation interruption starts (Fig. 1). To test this, a model-based analysis including variably saturated water flow was applied to simulate the transport of two nonreactive tracers applied either with irrigation water (^3H_2O) or with slurry (Br^-) in undisturbed loam soil columns injected with slurry. Simulated mass exchange was compared for continuous and intermittent irrigation regimes based on previously described soil column percolation experiments (Glæsner et al., 2011c). The comparison with a detailed three-dimensional (3D) model of transport of injected slurry solutes was used to verify if spatially localized injection can be described with a simplified one-dimensional (1D) double-porosity approach. The central aim was to explain the underlying mechanisms of leaching losses of nonreactive slurry components by double-porosity water and solute mass transfer.

Materials and Methods

Experimental Design

This study dealt with undisturbed loam soil columns (20 cm in diameter, 18–20 cm high; approximately 6000 cm^3) excavated from the plow layer of an agricultural field in Jutland, Aarup, Denmark. Mean values (n = 8) of soil physicochemical characteristics of 100-cm^3 cores included 19.7 g kg^{-1} total C, 1.5 g cm^{-3} bulk density, porosity of 0.45 cm^3 cm^{-3}, particle size distribution

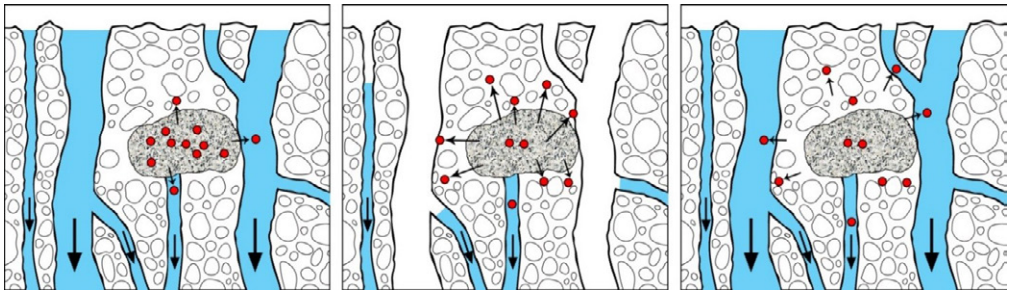

Fig. 1. Conceptual sketch illustrating the local nonequilibrium assumption and mass exchange from injected slurry (gray mass) during intermittent irrigation. The nonreactive soluble components of the slurry (red dots) are moving toward and within the water-filled larger pores during irrigation (left); diffusive exchange continues during interruption when larger pores are drained (center); and vertical transport in larger pores starts again after irrigation continues (right).

of 23.0% clay, 38.8% silt, and 38.2% sand, and 7.7, 9.8, 5.1 and 77.4% pore diameters of >600, 100 to 600, 30 to 100, and <30 μm, respectively. This study was based on experimental data from Glæsner et al. (2011c). Nine undisturbed columns were excavated in spring 2009 and were all subjected to injection of slurry, among which three replicate columns were subjected to a continuous irrigation intensity of 2 mm h^{-1}, an intermittent irrigation intensity of 2 mm h^{-1}, and intermittent irrigation intensity of 10 mm h^{-1}, respectively (Glæsner et al., 2011c). One column with an intermittent irrigation intensity of 10 mm h^{-1} was excluded due to permanent ponding on the soil surface. All undisturbed soil columns, excavated at field capacity, were initially saturated from the bottom for 3 d and subsequently drained on tension tables to −100 cm at the bottom during 13 d. Dairy slurry (6.6% dry matter content) spiked with KBr (2.69 g L^{-1} KBr) was applied to the soil columns at Day 11 at an application rate of 25 Mg ha^{-1} (75 g). Injection placed the slurry in a 1-cm-wide and 10-cm-long strip, placed 5 cm from the edge of the cylinder and 8 cm below the soil surface (Supplemental Fig. S1). The strip was lightly covered with soil without intentionally mixing soil and slurry (Glæsner et al., 2011a).

At Day 13, the columns were transferred to a percolation setup, and irrigation was initiated for 2.5 h without applied suction at the bottom. After 2.5 h (the time when the first leachate was observed at the column bottom), a pressure head of −5 cm was imposed at the bottom to ensure unsaturated conditions. Irrigation continued for 3.5 to 5.2 d (corresponding to 100 mm or 1.3–1.4 pore volumes). For the columns subjected to intermittent irrigation, irrigation interruptions were introduced after an application of 12.5 mm of irrigation water, and each interruption lasted for 10 h. The bottom pressure head was decreased from −5 to −20 cm during irrigation interruptions. One column from each irrigation regime (replicate columns C2–2, I2–1, and I10–1, see Table 1) received a pulse of 2.5 mm of ^3H_2O solution after steady outflow was observed (within 1.25 h) and before the interruptions were initiated.

The columns were weighed when drained to −100 cm, to −5 cm, and after 2 wk oven drying at 105°C.

One-Dimensional Modeling Approaches

Single-Porosity Flow and Equilibrium Transport Model

The Richards equation for variably saturated flow was used for describing single-porosity equilibrium model (SP-EQ) water flow:

$$\frac{\partial \theta}{\partial t} = \frac{\partial}{\partial z}\left[K(h)\left(\frac{\partial h}{\partial z}+1\right)\right] \quad [1]$$

where h is the pressure head (cm), $K(h)$ is the hydraulic conductivity function (cm d^{-1}), t is time (d), and z is the vertical coordinate (cm) (positive upward). The soil hydraulic properties are described with the standard van Genuchten–Mualem formulation:

$$\theta(h) = \theta_r + \frac{\theta_s - \theta_r}{\left(1+|\alpha h|^n\right)^m} \quad [2]$$

$$K(h) = K_s S_e^{0.5}\left[1-\left(1-S_e^{1/m}\right)^m\right]^2 \quad [3]$$

where θ_s and θ_r (cm^3 cm^{-3}) are saturated and residual water content parameters; α (cm^{-1}), n (dimensionless), and $m = 1 - 1/n$ are empirical parameters; $S_e = (\theta - \theta_r)/(\theta_s - \theta_r)$ is the effective water content (dimensionless); and K_s is the saturated hydraulic conductivity (cm d^{-1}).

Solute transport is described using the standard convection–dispersion equation in the form

$$\frac{\partial \theta R c}{\partial t} = \frac{\partial}{\partial z}\left(\theta D \frac{\partial c}{\partial z}\right) - \frac{\partial q c}{\partial z} \quad [4]$$

Table 1. Soil hydraulic parameters for the intact soil columns. For the double-porosity parameters, values for α, n, and K_s were equal to those of the single-porosity parameters. The parameters θ_{s_im} and θ_{s_m} as well as θ_{r_im} and θ_{r_m} were obtained using a median value of $\beta = \theta_m/\theta = 0.6$ of the mobile pore water fraction obtained in CXTFIT (data not shown).

	Single-porosity parameters‡					Double-porosity parameters§				
Column†	θ_s	θ_r	α	n	K_s	θ_{s_m}	θ_{r_m}	θ_{s_im}	θ_{r_im}	α_w
	cm^3 cm^{-3}		cm^{-1}		cm d^{-1}	cm^3 cm^{-3}				d^{-1}
C2–1	0.430	0.330	0.124	1.302	108	0.172	0.132	0.258	0.198	0.010
C2–2	0.410	0.310	0.124	1.302	108	0.164	0.124	0.246	0.186	0.052
C2–3	0.410	0.318	0.124	1.302	108	0.164	0.127	0.246	0.191	0.010
I2–1	0.395	0.305	0.124	1.302	108	0.158	0.122	0.237	0.183	0.552
I2–2	0.408	0.299	0.124	1.302	108	0.163	0.120	0.245	0.179	0.196
I2–3	0.418	0.315	0.124	1.302	108	0.167	0.126	0.251	0.189	0.036
I10–1	0.405	0.319	0.124	1.302	108	0.162	0.128	0.243	0.191	0.065
I10–2	0.410	0.340	0.124	1.302	108	0.164	0.136	0.246	0.204	0.156

† C2, continuous irrigation at 2 mm h^{-1}; I2, intermittent irrigation at 2 mm h^{-1}; I10, intermittent irrigation at 10 mm h^{-1}. Numbers after the dash represent column replicates.
‡ θ_s and θ_r, saturated and residual soil water content, respectively; α and n, van Genuchten shape parameters; K_s, saturated hydraulic conductivity.
§ Subscripts *m* and *im*, mobile and immobile fractions, respectively; α_w, water mass exchange coefficient.

where D is the effective dispersion coefficient ($cm^2\ d^{-1}$), R (dimensionless) is the retardation factor (we assumed conservative tracer transport using $R = 1$), c is the solute concentration ($g\ L^{-1}$), and q is the volumetric water flux density ($cm\ d^{-1}$) evaluated with the flow equation. Neglecting molecular diffusion in water, D is defined as

$$D = \lambda \frac{q}{\theta} \quad [5]$$

where λ is the dispersivity (cm). The dimensionless time, T, required to exchange one pore volume (PV) is given by

$$T = \frac{\theta L}{q} \quad [6]$$

where L is the transport distance or, here, the column length (cm).

Double-Porosity Mobile–Immobile Flow and Transport Model

The double-porosity and mobile–immobile approaches partition the bulk soil into fractions for mobile (subscript *m*) and immobile (subscript *im*) pore-water regions for the volumetric water content, θ, and the solute mass as $\theta = \theta_{im} + \theta_m$ and $c\theta = c_{im}\theta_{im} + c_m\theta_m$, respectively. The water flow in a soil with mobile and immobile pore water regions is described as (Šimůnek et al., 2003)

$$\frac{\partial \theta_m(h_m)}{\partial t} = \frac{\partial}{\partial z}\left[K(h_m)\left(\frac{\partial h_m}{\partial z}\right)+1\right]-\Gamma_w \quad [7a]$$

$$\frac{\partial \theta_{im}(h_{im})}{\partial t} = \Gamma_w \quad [7b]$$

where the hydraulic conductivity, K, is only defined for the mobile pore water region, and the water exchange rate, Γ_w (d^{-1}), depends on the difference in pressure heads

$$\Gamma_w = \alpha_w(h_m - h_{im}) \quad [8]$$

where α_w is the first-order water mass exchange coefficient (d^{-1}).

Solute transport in the DP-MIM model is considered here (i.e., no sorption) as

$$\frac{\partial \theta_m c_m}{\partial t} = \frac{\partial}{\partial z}\left(\theta_m D_m \frac{\partial c_m}{\partial z}\right) - \frac{\partial q_m c_m}{\partial z} - \Gamma_s \quad [9a]$$

$$\frac{\partial \theta_{im} c_{im}}{\partial t} = \Gamma_s \quad [9b]$$

where D_m and q_m are both defined for the mobile pore water region, and Γ_s is the solute mass exchange rate ($g\ L^{-1}\ d^{-1}$), defined as

$$\Gamma_s = \alpha_s(c_m - c_{im}) + \Gamma_w c^* \quad [10]$$

where α_s is the mass exchange coefficient for solutes (d^{-1}); this solute mass exchange term is described depending on a combination of both the concentration difference (first term) and the advective exchange (second term), in which the solute concentration, c^*, depends on the direction of the water exchange (see above, Eq. [8]).

One-Dimensional Initial and Boundary Conditions

For slurry injection, we assumed the slurry and Br^- to be fully mixed with the soil in a vertical layer of 7-cm thickness at a 4- to 11-cm soil depth. The full mixing of slurry and soil in the layer was required when assuming a 1D vertical model. This application-induced increase in water contents was considered to be limited by the available water storage porosity or air-filled porosity at the time of application; hence the vertical thickness of the injection layer was calculated as the soil volume that could store the added slurry water without exceeding the experimentally determined porosity.

Upper boundary conditions in the HYDRUS-1D program (Version 4.16.0110; Šimůnek et al., 2016) were set to atmospheric with a surface layer. The lower boundary was set to a pressure head of −100 cm during drainage. A seepage face condition of 0 cm (i.e., to consider atmospheric pressure in the air-filled funnel) was imposed at the bottom boundary when irrigation was initiated. Thereafter, a seepage face condition of −5 cm was imposed after 2.5 h as air pressure was applied directly at the bottom boundary at this time (see above). Note that a pressure head instead of a seepage face condition would have induced an uptake of water from the bottom boundary, which is opposite to observations. The changes in the bottom boundary were required to split the simulation runs in a series of three interrupted model periods per column, because HYDRUS-1D Version 4.16.0110 does not allow a change in time of the type of boundary condition (from pressure head to seepage face) or the pressure head value of the seepage face. Hence, the final conditions of a previous period were applied as the initial conditions in the subsequent period during each simulation run.

The application of ^3H_2O was described as a concentration flux at the upper boundary and a zero concentration gradient at the lower boundary, whereas the application of Br^- in the injected slurry was represented as an initial condition of the Br^- resident concentration. For the initial model period simulation, we assumed that the concentration in the immobile pore water region was in equilibrium with that of the pore water in the mobile region, whereas for the simulations of the subsequent model period, calculated distributions of concentrations in the two pore regions were used.

Soil Hydraulic Model Parameters

From the experimental conditions (Glæsner et al., 2011c), the volumetric water contents at −5 and −100 cm from each 6000-cm^3 undisturbed soil column as well as eight values of the water retention curve from 100-cm^3 undisturbed core samples were available in the pressure head range between −5 and −300 cm. An initial set of van Genuchten–Mualem parameters was obtained using the ROSETTA program (Schaap et al., 2001) implemented in HYDRUS from values of bulk texture, bulk density, and water content at −330 cm for each soil texture; note that we used the value at −100 cm for the −330-cm step, but this was only as an initial estimate. In a first step, these initial estimates of the van Genuchten–Mualem curves were improved in the experimental pressure head range by fitting the eight retention values of the

100-cm^3 cores using the RETC program (van Genuchten et al., 1991). In a second step, the α and n parameters were kept fixed, and values for θ_r, θ_s, and K_s were adjusted to match the hydraulic properties of the large columns by using data from water retention and steady-state flow measurements. More specifically, the three parameters were further adjusted to match the average water content of the large columns at $h = -5$ and -100 cm, respectively, and the hydraulic conductivity for $h = -5$ cm. The value of $K(-5$ cm) was set equal to the applied steady-state rate of 2 mm h^{-1}.

For the DP-MIM, the same values of α and n were used and assumed identical for both mobile and immobile pore water regions to reduce the number of parameters to be identified. We assumed that the mobile pore water region represented 40% of the total volume, based on initial fitting of ^3H_2O-tracer breakthrough curves (BTCs) using the CXTFIT program (Toride et al., 1995) as implemented in STANMOD software (Šimůnek et al., 2008) (not shown).

Solute Transport and Mass Exchange Parameters

The initial dispersivity parameter, λ, was obtained by fitting a ^3H_2O BTC using the CXTFIT program. The values of λ were used as initial estimates and fitted for ^3H_2O and Br^- solute transport parameters in HYDRUS-1D.

Values of the solute exchange coefficient, α_s, from Eq. [10] were additionally obtained by fitting a ^3H_2O BTC using the CXTFIT program, used as initial estimates, and fitted for ^3H_2O and Br^- solute transport parameters in HYDRUS-1D.

Values of the water exchange coefficient, α_w, from Eq. [8] in DP-MIM were estimated in HYDRUS-1D using an initial value of 0.01 d^{-1}. Estimated values of α_w varied between 0.01 and 0.552 d^{-1} (Table 1). For Columns C2–1 and C2–3, the value of α_w was fixed to the initial value (i.e., 0.01 d^{-1}) to avoid numerical problems.

HYDRUS-3D

Based on the calibrated 1D model, we ran 3D simulations using HYDRUS-3D (Šimůnek et al., 2016) for an initial slurry distribution in a volume of 1 by 1 by 10 cm located 8 cm below the column surface (Supplemental Fig. S1), based on the experimental conditions. Comparisons between 1D and fully 3D simulations were conducted for both equilibrium and nonequilibrium models and for both continuous and intermittent water application.

Quantitative Model Comparison

The two modeling approaches were compared based on the root mean square error (RMSE) between experimental data and model predictions for the equilibrium and mobile–immobile models (Bennett et al., 2013). The RMSE is given by

$$\mathrm{RMSE} = \sqrt{\frac{1}{\mathrm{nn}}\sum_{i=1}^{\mathrm{nn}}\left(C_i - \hat{C}_i\right)^2} \qquad [11]$$

where nn is the number of observations and C_i and $\hat{C}_i$ are the measured and simulated concentrations, respectively.

Results and Discussion

Model Parameterization and Scenario Selection

The estimated model parameters (Table 1) could simulate the experimental observations well; the simulated water contents matched the measured water contents of the undisturbed columns during the initial drainage period (Day 1–13) and at the end of irrigation (Fig. 2A). A similar match was obtained for the water outflow during irrigation and during irrigation interruptions (Fig. 2B and 2C).

Fitted BTCs of the two solutes during continuous irrigation are shown in Fig. 3A and 4A to 4C. The estimated solute transport parameters for ^3H_2O were in the same order of magnitude for the estimated Br^- parameters (Table 2), which is reflected in the fact that both solutes are nonreactive. The dispersivity (λ) obtained by SP-EQ was higher than from DP-MIM (Table 2), as some of the solute spreading included in the dispersivity using SP-EQ is explained by solute exchange between mobile and immobile regions in the DP-MIM. Estimated dispersivity was in the range of values reported by others for similar soil types (Köhne et al., 2004; Vanderborght and Vereecken, 2007).

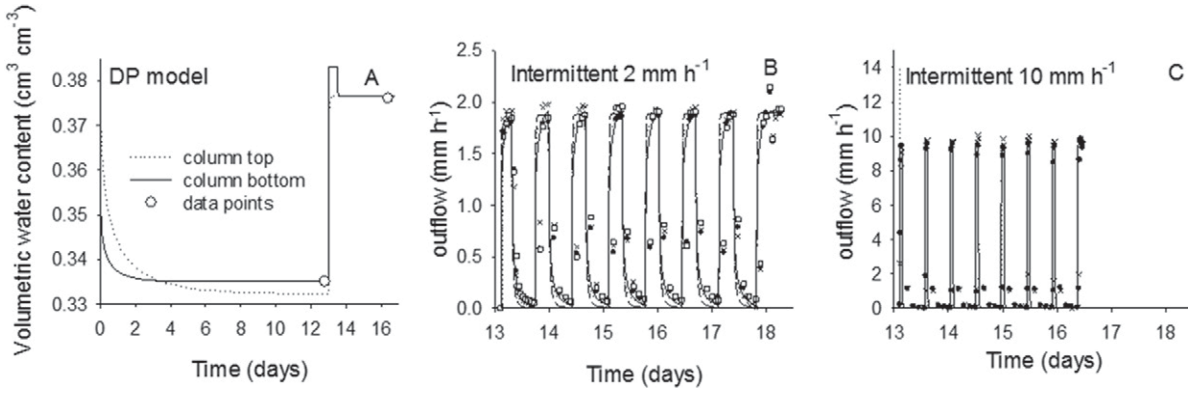

Fig. 2. (A) Water contents in the top (dotted lines) and bottom (solid lines) nodes simulated by the dual-porosity (DP) model at the boundaries of soil columns after removal from wetting (Day 0) during the experimental period of continuous irrigation, after slurry was applied at Day 11 and irrigation started at Day 13; water outflow of replicate columns during intermittent irrigation at (B) 2 mm h^{-1} and (C) 10 mm h^{-1}. Note different range on *y* axis. Symbols represent data, and lines represent simulations applying the double-porosity mobile–immobile model in HYDRUS-1D.

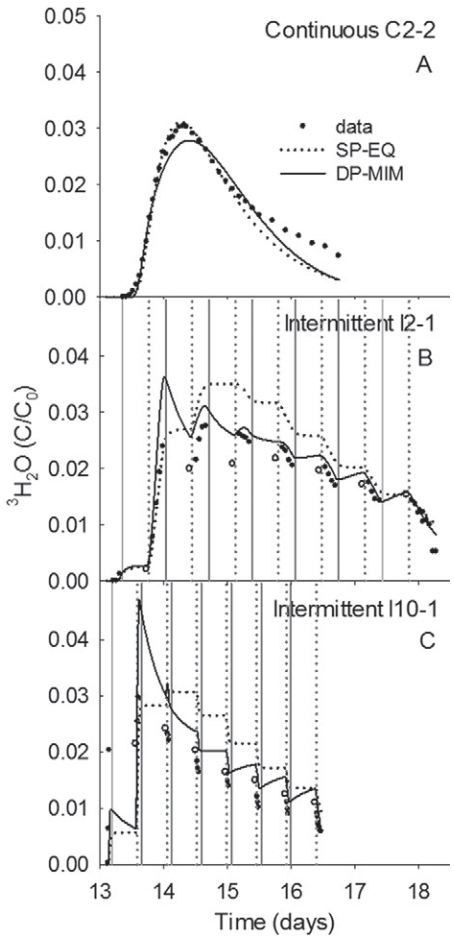

Fig. 3. Measured and simulated ^3H_2O breakthrough curves during (A) continuous irrigation at 2 mm h^{-1} (C2-2) and intermittent irrigation at (B) 2 mm h^{-1}(I2-1) and (C) 10 mm h^{-1} (I10-1). Samples collected during flow are indicated by solid symbols and open symbols indicate samples collected during interruptions; vertical solid lines represent times of interruptions and vertical dotted lines initiation of irrigation. Model simulations using HYDRUS-1D are represented by lines: single-porosity flow and equilibrium transport (SP-EQ, dotted) and double-porosity mobile–immobile (DP-MIM, solid).

The 3D simulation results included the physically realistic description of the redistribution of solutions in all directions from the application strip. The comparison with the simplified 1D simulations showed that the assumed layered application in one dimension was sufficient to produce similar breakthrough curves (Supplemental Fig. S2).

Surface-Applied Nonreactive Tracer

The DP-MIM described ^3H_2O leaching (applied with irrigation water) during intermittent irrigation conditions better than the simpler SP-EQ (Fig. 3), mainly because solute and water exchange was included in the DP-MIM. When pores are draining during flow interruptions, the local concentration and pressure head gradients change within the soil, which is accounted for by the additional exchange of solute and water in DP-MIM. Calculated RMSE values were consistently lower for DP-MIM than for SP-EQ (Table 2), and due to the equilibrium assumption in the SP-EQ, this model cannot capture increasing concentrations during irrigation interruptions.

Dispersivity (λ) increased when the irrigation intensity increased under intermittent conditions (Table 2, Columns I2–1 and I10–1). The increase of dispersivity with irrigation intensity has previously been reported for unsaturated flow in fine-textured soils and explained by the activation of larger pores when the leaching rate exceeds the conductivity of the smaller pores (Vanderborght and Vereecken, 2007).

The DP-MIM predicted water exchange from mobile to immobile (positive values) pore regions during irrigation and vice versa (descending curves) during irrigation interruptions in the intermittent irrigation experiments (Fig. 5A), as also described by others (Köhne et al., 2004; Gerke et al., 2013) and hypothesized in the conceptual model (Fig. 1). Despite the cumulative water exchange from the intermittent irrigation fluctuations during irrigation and irrigation interruptions, the cumulative water exchange was in the same range as for the continuous irrigation regime at the same irrigation intensity (Fig. 5A). The temporal fluctuations in the cumulative water exchange during intermittent irrigation are less evident in the cumulative exchange curve of the nonreactive tracer, ^3H_2O (Fig. 5B). This indicates that "diffusive" mass exchange of ^3H_2O caused by concentration differences between mobile and immobile pore regions was the quantitatively dominating mechanism for ^3H_2O exchange compared with "advective" exchange of ^3H_2O with water caused by local pressure head differences. After one eluted PV, higher cumulative exchange of ^3H_2O was recorded for intermittent irrigation (Fig. 5B; 1 PV = 48.18 Bq cm^{-2}) compared with continuous irrigation (Fig. 5B; 1 PV = 25.93 Bq cm^{-2}). This corresponds to a lower mass recovery of leached ^3H_2O recorded during intermittent (at 1.25 PV, 76.4%; Glæsner et al., 2011c) than continuous (at 1.25 PV, 86.6%; Glæsner et al., 2011c) irrigation at the same irrigation intensity (2 mm h^{-1}). The role of larger cumulative mass exchange from mobile to immobile pore regions under intermittent conditions has also been reported in other studies (e.g., Brusseau et al., 1997).

When increasing the irrigation intensity (10 mm h^{-1}), mass recovery of leached ^3H_2O was lower than at 2 mm h^{-1} (at 1.25 PV, 72.1%; Glæsner et al., 2011c), even though the model simulated a similar cumulative mass exchange to intermittent irrigation at the lower irrigation intensity (Fig. 5B; 1 PV = 50.1 Bq cm^{-2}). This confirms that mass exchange of the irrigation-applied tracer from mobile to immobile pore regions was mainly induced by concentration gradients rather than pressure head gradients because the water mass exchange was much lower for the high irrigation intensity (Fig. 5A).

Nonreactive Tracer Placed within the Soil

The DP-MIM also described Br^- leaching (applied with injected slurry) under intermittent irrigation conditions better than the simpler SP-EQ model (Fig. 4). This is shown by the lower RMSE in the case of DP-MIM (except for C2–2) (Table 2), and, as mentioned above for the ^3H_2O data, the SP-MIM failed to show

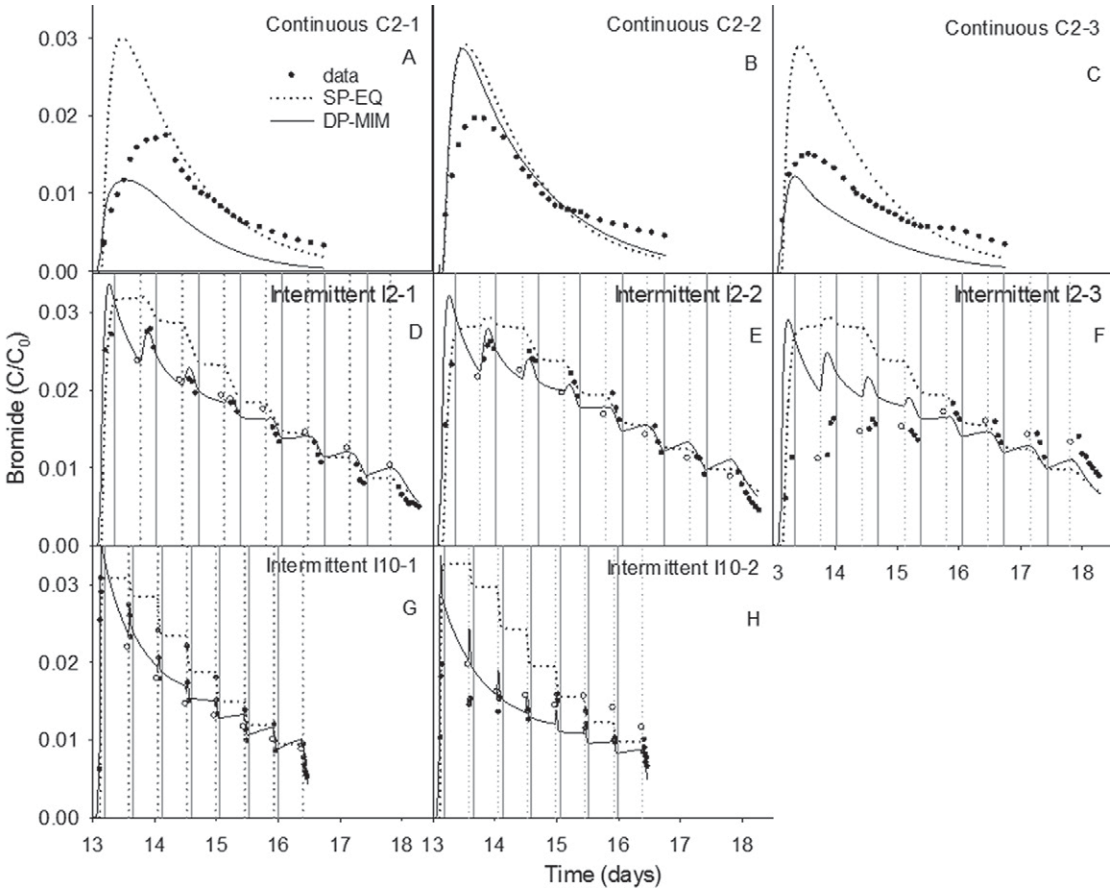

Fig. 4. Measured and simulated Br^- breakthrough curves during continuous irrigation at 2 mm h^{-1} (C2) and intermittent irrigation at 2 (I2) and 10 mm h^{-1} (I10). Samples collected during flow are indicated by solid symbols and open symbols indicate samples collected during interruptions; vertical solid lines represent interruptions and vertical dotted lines represent initiation of irrigation. Model simulations using HYDRUS-1D are represented by lines: single-porosity flow and equilibrium transport (SP-EQ, dotted) and double-porosity mobile–immobile (DP-MIM, solid).

increasing Br^- concentrations during irrigation interruptions. The Br^- mass exchange values were all negative (Fig. 5C), indicating that exchange of injected Br^- is directed only from the immobile to the mobile pore water region. This exchange characteristic of solutes from injected slurry corresponds well with Br^- being placed within the undisturbed soil columns at a suction of −100 cm, when only pores smaller than 30 μm are water filled according to the Young–Laplace equation. Although the water content of the slurry increased the number of pore size classes being saturated, Br^- could be assumed to quickly diffuse into the water-filled pore space (i.e., the immobile pore water region) at the time of application.

A simulation example of water content distributions using DP-MIM shows that mobile pore water rapidly distributed evenly throughout the soil profile after slurry injection (Fig. 6). Water contents changed more slowly in the immobile pore water region and became evenly distributed in the vertical direction after 1 d of irrigation (i.e., Day 14 in Fig. 6). The Br^- concentration distribution remained close to that of the initial distribution before irrigation was initiated; after irrigation (Day 14), the Br^- concentration in the mobile region quickly approached a relatively uniform vertical distribution. The distribution of the Br^- concentration in the immobile region changed more slowly after irrigation

Table 2. Estimated dispersivity parameter, λ, and solute exchange parameter, α_s, for ^3H_2O and Br^- obtained in HYDRUS-1D using the single-porosity flow and equilibrium transport (SP-EQ) and the double-porosity mobile–immobile (DP-MIM) models for all columns.

	SP-EQ		DP-MIM		
Column†	λ	RMSE	λ	α_s	RMSE
	cm		cm	d^{-1}	
C2–2	4.70 ± 0.01‡	0.0021	1.20 ± 0.51	0.997 ± 0.24	0.0021
I2–1	6.88 ± 0.06	0.0053	2.22 ± 0.57	0.246 ± 0.03	0.0041
I10–1	9.75 ± 0.09	0.0079	3.12 ± 0.83	0.255 ± 0.04	0.0069
C2–1	7.32 ± 0.14	0.0076	4.04 ± 5.22	0.312 ± 0.88	0.0048
C2–2	7.05 ± 0.07	0.0046	3.71 ± 2.26	0.281 ± 0.36	0.0049
C2–3	9.58 ± 0.16	0.0064	1.21 ± 4.28	0.395 ± 0.09	0.0039
I2–1	9.55 ± 0.03	0.0030	3.45 ± 0.85	0.142 ± 0.03	0.0017
I2–2	8.10 ± 0.03	0.0035	3.91 ± 1.77	0.193 ± 0.05	0.0031
I2–3	9.33 ± 0.38	0.0077	6.33 ± 2.99	0.184 ± 0.12	0.0063
I10–1	10.8 ± 0.03	0.0042	2.26 ± 1.07	0.176 ± 0.04	0.0030
I10–2	10.3 ± 0.27	0.0080	6.19 ± 2.30	0.135 ± 0.10	0.0057

† C2, continuous irrigation at 2 mm h^{-1}; I2, intermittent irrigation at 2 mm h^{-1}; I10, intermittent irrigation at 10 mm h^{-1}. Numbers after the dash represent column replicates.
‡ Estimated values ± standard error of the nonlinear least-squares analysis.

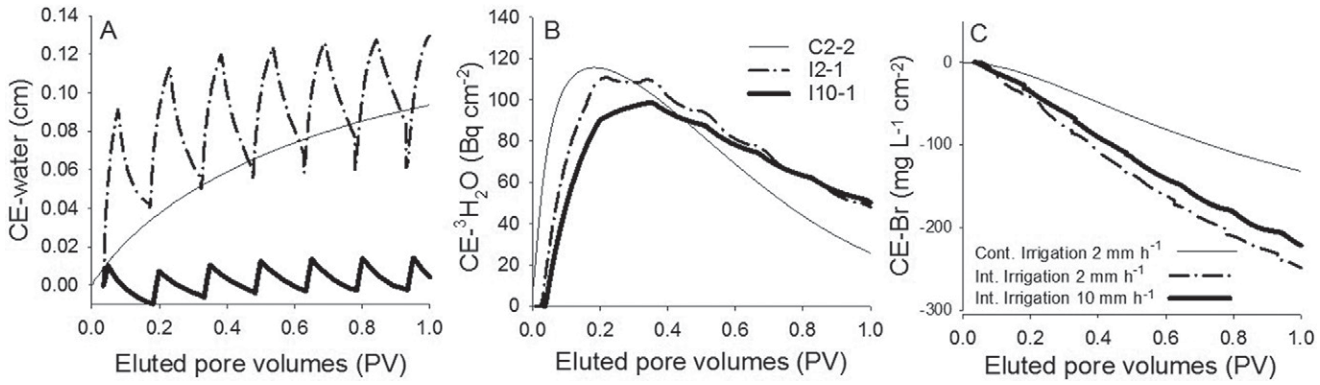

Fig. 5. Cumulative exchange (CE) of (A) water, (B) ^3H_2O, and (C) Br^- during continuous irrigation at 2 mm h^{-1} (C2) and intermittent irrigation at 2 (I2) and 10 mm h^{-1} (I10) for slurry injection simulated with the dual-porosity mobile–immobile (DP-MIM) model until one eluted PV. For water and Br^-, average values of the replicate columns are shown, whereas for ^3H_2O, the columns receiving ^3H_2O are shown.

was initiated, and a larger fraction of Br^- remained within the immobile region (Fig. 6).

Mass recovery of leached Br^- during continuous irrigation (at 1.25 PV, 45.5 ± 2.5%; Glæsner et al., 2011c) was found to be lower than during intermittent irrigation (at 1.25 PV, 59.3 ± 5.2%; Glæsner et al., 2011c) at the same irrigation intensity (2 mm h^{-1}). This experimental finding corresponds well with the simulated higher cumulative mass exchange from immobile to mobile pore regions during intermittent irrigation (Fig. 5C; 1 PV = −248 mg L^{-1} cm^{-2}) compared with continuous irrigation (Fig. 5C; 1 PV = −132 mg L^{-1} cm^{-2}) as conceptualized in Fig. 1, thereby resulting in higher effluent mass recovery for intermittent irrigation. The distribution of Br^- during injection and irrigation compared with Fig. 6 is visualized in the 3D Supplemental Video. It demonstrates that Br^- mass exchange from immobile to mobile pore regions occurs during interruptions and that Br^- is leached on resuming irrigation. This mechanism further explains the higher effluent concentrations following rainwater interruptions (Fig. 4), as was also found elsewhere (e.g., Wehrer and Totsche, 2005).

As the irrigation intensity increased (10 mm h^{-1}), the mass recovery of Br^- decreased (at 1.25 PV, 55.3 ± 5.4%) (Glæsner et al., 2011c), which was supported by the slightly lower cumulative mass exchange of Br^- (Fig. 5C; 1 PV = −219 mg L^{-1} cm^{-2}) than during irrigation at 2 mm h^{-1} (Fig. 5C; 1 PV = −248 mg L^{-1} cm^{-2}).

This study indicates that accurate prediction of nutrient fate at the field scale requires the use of more advanced numerical models, like the double-porosity model. However, transferring information from the laboratory scale to the field scale is prone to error due to the divergence of physical processes between different spatial scales. For this reason, application of more advanced numerical models at the field scale requires a new parameterization based on field experiments.

Conclusions

The role of solute mass exchange was analyzed using single- and double-porosity models implemented in HYDRUS. Both single- and double-porosity water flow and mobile–immobile solute transport models described the data well. However, as experimental conditions became more complex (variably saturated flow),

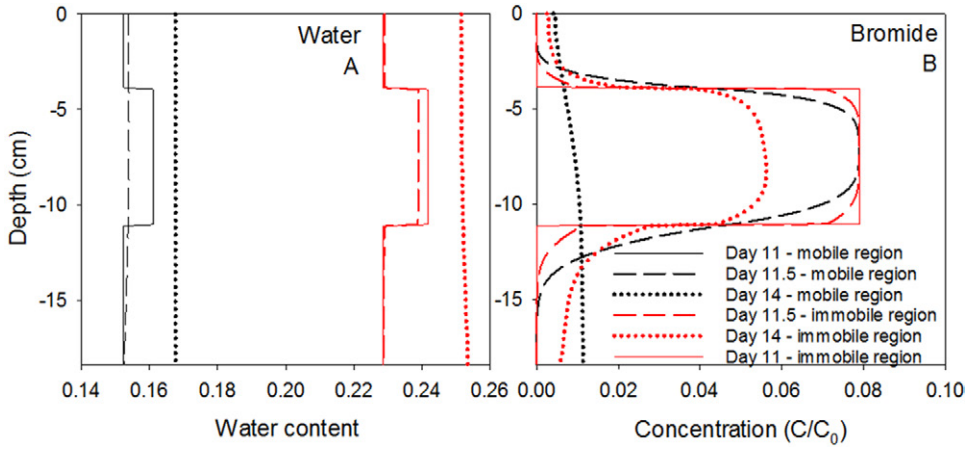

Fig. 6. Effects of initial conditions for describing (A) water and (B) Br^- distribution after slurry injection in the one-dimensional model and dual-porosity mobile–immobile approach. In (B) at Day 11, we assumed that the concentration in the immobile pore water region was in equilibrium with that of the pore water in the mobile region; therefore the two lines overlap each other.

the DP-MIM described the data even better by considering solute and water exchange between pore regions.

Introducing rainfall interruptions with variably saturated, intermittent soil water movement led to higher leaching of injected slurry compounds compared with steady-flow conditions (Glæsner et al. 2011c). The current model-based analysis could explain this by an increased mass exchange of dissolved injected slurry components from the immobile to the mobile pore water regions during interruptions. The exchange coefficients are in realistic ranges, suggesting that local-scale mass exchange affected the solute concentration in leachates. The results highlight the importance of selecting experimental conditions more similar to natural conditions (i.e., rainfall interruptions) when striving to obtain improved understanding of nutrient leaching after slurry application, as local (pore-scale) processes affect larger scale leaching losses. Column tests under steady-flow conditions could lead to underestimations of solute leaching after slurry injection in structured soils. Thus, local-scale mass exchange processes should be included in model predictions of nutrient losses from agricultural fields.

Variables

c solute concentration (g L^{-1})
$_c\theta$ solute mass
D dispersion coefficient (cm^2 d^{-1})
K_s saturated hydraulic conductivity (cm d^{-1})
$K(h)$ unsaturated hydraulic conductivity function (cm d^{-1})
L column length (cm)
R retardation factor, dimensionless
S_e effective water content, dimensionless
S_e^{im} effective water content, immobile region (Šimůnek et al., 2003)
S_e^{m} effective water content, mobile region (Šimůnek et al., 2003)
T dimensionless time of a pore volume
h pressure head (cm)
m van Genuchten–Mualem parameter
n van Genuchten–Mualem parameter
l van Genuchten–Mualem parameter
q volumetric water flux density (cm d^{-1}) (Eq. [6])
t time (d^{-1})
v pore water velocity (cm d^{-1})
z vertical coordinate, depth (cm)
α van Genuchten–Mualem parameter (cm^{-1})
α_s first order solute mass exchange coefficient (d^{-1}) (Eq. [7])
α_w first order water mass exchange coefficient (d^{-1})
β partitioning coefficient mobile water fraction $\beta = \theta_m/\theta$, (Eq. [8])
λ dispersivity, dispersion length (cm)
θ water content SPM (cm^3 cm^{-3})
θ_{im} immobile water content (cm^3 cm^{-3})
θ_m mobile water content (cm^3 cm^{-3})
θ_r residual water content (cm^3 cm^{-3})
θ_{rm} residual water content, mobile pore water region (cm^3 cm^{-3})
θ_{rim} residual water content, immobile pore water region (cm^3 cm^{-3})
θ_s saturated water content (cm^3 cm^{-3})
θ_{sm} saturated water content, mobile pore water region (cm^3 cm^{-3})
θ_{sim} saturated water content, immobile pore water region (cm^3 cm^{-3})
Γ_s solute mass exchange rate (g L^{-1} d^{-1})
Γ_w water mass exchange rate (d^{-1})

Subscripts

m mobile pore water region
im immobile pore water region

Supplemental Information

Two supplements are provided. One supplement includes two figures, one showing the location of injected slurry in the soil columns (from HYDRUS-3D) and the other showing a comparison of simulated Br^- leaching for two columns using the 1D and 3D approaches. The second supplement is a 3D video of mobile and immobile Br^- concentrations during irrigation and irrigation interruptions, showing the mass exchange during irrigation interruptions.

Acknowledgments

The model analyses were carried out at the Leibniz Centre for Agricultural Landscape Redearch (ZALF) during a research stay financed by Villum Fonden, a part of the Velux Foundations.

References

Ball Coelho, B.R., R.C. Roy, E. Topp, and D.R. Lapen. 2007. Tile water quality following liquid swine manure application into standing corn. J. Environ. Qual. 36:580–587. doi:10.2134/jeq2006.0306

Bennett, N.D., B.F. Croke, G. Guariso, J.H. Guillaume, S.H. Hamilton, A.J. Jakeman, et al. 2013. Characterising performance of environmental models. Environ. Modell. Softw. 40:1–20. doi:10.1016/j.envsoft.2012.09.011

Brusseau, M.L., Q.H. Hu, and R. Srivastava. 1997. Using precipitation interruption to identify factors causing nonideal contaminant transport. J. Contam. Hydrol. 24:205–219. doi:10.1016/S0169-7722(96)00009-5

de Jonge, L.W., P. Moldrup, G.H. Rubæk, K. Schelde, and J. Djurhuus. 2004. Particle leaching and particle-facilitated transport of phosphorus at field scale. Vadose Zone J. 3:462–470. doi:10.2136/vzj2004.0462

Flühler, H., W. Durner, and M. Flury. 1996. Lateral solute mixing processes: A key for understanding field-scale transport of water and solutes. Geoderma 70:165–183.

Gerke, H.H. 2006. Preferential flow descriptions for structured soils. J. Plant Nutr. Soil Sci. 169:382–400. doi:10.1002/jpln.200521955

Gerke, H.H., J. Dusek, and T. Vogel. 2013. Solute mass transfer effects in two-dimensional dual-permeability modeling of bromide leaching from a tile-drained field. Vadose Zone J. 12(2). doi:10.2136/vzj2012.0091

Gerke, H.H., and M.Th. van Genuchten. 1993. A dual-porosity model for simulating the preferential movement of water and solutes in structured porous media. Water Resour. Res. 29:305–319. doi:10.1029/92WR02339

Giola, P., B. Basso, G. Pruneddu, F. Giunta, and J.W. Jones. 2012. Impact of manure and slurry applications on soil nitrate in a maize–triticale rotation: Field study and long term simulation analysis. Eur. J. Agron. 38:43–53. doi:10.1016/j.eja.2011.12.001

Glæsner, N., E. Donner, J. Magid, G.H. Rubæk, H. Zhang, and E. Lombi. 2012. Characterization of leached phosphorus from soil, manure, and manure-amended soil by physical and chemical fractionation and diffusive gradients in thin films (DGT). Environ. Sci. Technol. 46:10564–10571. doi:10.1021/es301861a

Glæsner, N., C. Kjaergaard, G.H. Rubæk, and J. Magid. 2011a. Interacting effects of soil texture and placement of dairy slurry application: I. Flow characteristics and leaching of nonreactive components. J. Environ. Qual. 40:337–343. doi:10.2134/jeq2010.0317

Glæsner, N., C. Kjaergaard, G.H. Rubæk, and J. Magid. 2011b. Interacting effects of soil texture and placement of dairy slurry application: II. Leaching of phosphorus forms. J. Environ. Qual. 40:344–350. doi:10.2134/jeq2010.0318

Glæsner, N., C. Kjaergaard, G.H. Rubæk, and J. Magid. 2011c. Effect of irrigation regimes on mobilization of nonreactive tracers and dissolved and particulate phosphorus in slurry-injected soils. Water Resour. Res. 47:W12536. doi:10.1029/2011WR010769

Jarvis, N. 1994. The MACRO model (version 3.1): Technical description and sample simulations. Rep. Diss. 19. Dep. of Soil Sci., Swedish Univ. of Agric. Sci., Uppsala.

Jarvis, N.J. 2007. A review of non-equilibrium water flow and solute transport in soil macropores: Principles, controlling factors and consequences for water quality. Eur. J. Soil Sci. 58:523–546.

Köhne, M.J., S. Köhne, B.P. Mohanty, and J. Šimůnek. 2004. Inverse mobile–immobile modeling of transport during transient flow: Effects of between-domain transfer and initial water content. Vadose Zone J. 3:1309–1321. doi:10.2136/vzj2004.1309

Kronvang, B., G.H. Rubæk, and G. Heckrath. 2009. International Phosphorus Workshop: Diffuse phosphorus loss to surface water bodies–Risk assessment, mitigation options and ecological effects in river basins. J. Environ. Qual. 38:1924–1929. doi:10.2134/jeq2009.0051

Liu, J., H. Aronsson, B. Ulen, and L. Bergström. 2012. Potential phosphorus leaching from sandy topsoils with different fertilizer histories before and after application of pig slurry. Soil Use Manage. 28:457–467. doi:10.1111/j.1475-2743.2012.00442.x

Maguire, R.O., P.J.A. Kleinman, C.J. Dell, D.B. Beegle, R.C. Brandt, J.M. McGrath, and Q.M. Ketterings. 2011. Manure application technology in reduced tillage and forage systems: A review. J. Environ. Qual. 40:292–301. doi:10.2134/jeq2009.0228

Pain, B., and H. Menzi. 2003. Glossary of terms on livestock manure management 2003. Recycling Agricultural, Municipal, and Industrial Residues in Agriculture Network, Swiss College of Agriculture, Zollikofen, Switzerland. http://www.ramiran.net/DOC/Glossary2003.pdf

Rubæk, G.H., K. Henriksen, J. Petersen, B. Rasmussen, and S.G. Sommer. 1996. Effects of application method and anaerobic digestion on gaseous nitrogen loss from animal slurry applied to ryegrass (*Lolium perenne*). J. Agric. Sci. 126:481–492. doi:10.1017/S0021859600075572

Schaap, M.G., F.J. Leij, and M.Th. van Genuchten. 2001. ROSETTA: A computer program for estimating soil hydraulic parameters with hierarchical pedotransfer functions. J. Hydrol. 251:163–176. doi:10.1016/S0022-1694(01)00466-8

Šimůnek, J., N.J. Jarvis, M.Th. van Genuchten, and A. Gärdenäs. 2003. Review and comparison of models for describing non-equilibrium and preferential flow and transport in the vadose zone. J. Hydrol. 272:14–35. doi:10.1016/S0022-1694(02)00252-4

Šimůnek, J., and M.Th. van Genuchten. 2008. Modeling nonequilibrium flow and transport processes using HYDRUS. Vadose Zone J. 7:782–797. doi:10.2136/vzj2007.0074

Šimůnek, J., M.Th. van Genuchten, and M. Šejna. 2008. Development and applications of the HYDRUS and STANMOD software packages and related codes. Vadose Zone J. 7:587–600. doi:10.2136/vzj2007.0077

Šimůnek, J., M.Th. van Genuchten, and M. Šejna. 2016. Recent developments and applications of the HYDRUS computer software packages. Vadose Zone J. 15(7). doi:10.2136/vzj2016.04.0033

Toride, N., F.J. Leij, and M.Th. van Genuchten. 1995. The CXTFIT code for estimating transport parameters from laboratory or field tracer experiments. Version 2.0. Res. Rep. 137. US Salinity Lab., Riverside, CA.

Vanderborght, J., and H. Vereecken. 2007. Review of dispersivities for transport modeling in soils. Vadose Zone J. 6:29–52. doi:10.2136/vzj2006.0096

van Genuchten, M.Th., and F.N. Dalton. 1986. Models for simulating salt movement in aggregated field soils. Geoderma 38:165–183. doi:10.1016/0016-7061(86)90013-3

van Genuchten, M.Th., F.J. Leij, and S.R. Yates. 1991. The RETC code for quantifying the hydraulic functions of unsaturated soils. Version 1.0. USEPA Rep. 600/2-91/065. US Salinity Lab., Riverside, CA.

van Genuchten, M.Th., and P.J. Wierenga. 1976. Mass-transfer studies in sorbing porous media: 1. Analytical solutions. Soil Sci. Soc. Am. J. 40:473–480. doi:10.2136/sssaj1976.03615995004000040011x

Webb, J., B. Pain, S. Bittman, and J. Morgan. 2010. The impacts of manure application methods on emissions of ammonia, nitrous oxide and on crop response: A review. Agric. Ecosyst. Environ. 137:39–46. doi:10.1016/j.agee.2010.01.001

Wehrer, M., and K.U. Totsche. 2005. Determination of effective release rates of polycyclic aromatic hydrocarbons and dissolved organic carbon by column outflow experiments. Eur. J. Soil Sci. 56:803–813.